Use of recycled tyre segments to enhance the stability of ballasted track by increased confinement

Soumyaranjan Mishra

PhD student, Transport Research Centre, School of Civil and Environmental Engineering, University of Technology Sydney, Ultimo, Sydney, Australia; and ARC Industrial Transformation Training Centre for Advanced Technologies in Rail Track Infrastructure (ITTC-Rail).

Buddhima Indraratna, PhD (Alberta), FTSE, FIEAust, FASCE, FGS

Distinguished Professor of Civil Engineering and Director of Transport Research Centre, University of Technology Sydney, Ultimo, Australia; Founding Director, ARC Industrial Transformation Training Centre for Advanced Technologies in Rail Track Infrastructure (ITTC-Rail)

Cholachat Rujikiatkamjorn, PhD, MASCE

Professor, Transport Research Centre School of Civil and Environmental Engineering, University of Technology Sydney, Ultimo, NSW 2007, Australia

Trung Ngo, PhD, MASCE

Senior lecturer, Transport Research Centre, School of Civil and Environmental Engineering, University of Technology Sydney, Ultimo, Australia.

Author for correspondence:

Distinguished Professor Buddhima Indraratna

Transport Research Centre

University of Technology Sydney

Ultimo, NSW 2007

Australia.

Ph: +61 2 9514 8000

Email: buddhima.indraratna@uts.edu.au

1

Use of recycled tyre segments to enhance the stability of ballasted track by increased confinement

Authors: Soumyaranjan Mishra[a], Buddhima Indraratna[b], Cholachat Rujikiatkamjorn[c], Trung Ngo[d]

[a]PhD student, Transport Research Centre, School of Civil and Environmental Engineering, University of Technology Sydney, Ultimo, Sydney, Australia; and ARC Industrial Transformation Training Centre for Advanced Technologies in Rail Track Infrastructure (ITTC-Rail). Email: Soumyaranjan.Mishra@student.uts.edu.au

[b]Distinguished Professor of Civil Engineering and Director of Transport Research Centre, University of Technology Sydney, Ultimo, Australia; Founding Director, ARC Industrial Transformation Training Centre for Advanced Technologies in Rail Track Infrastructure (ITTC-Rail). Email: buddhima.indraratna@uts.edu.au

[c]Professor, Transport Research Centre School of Civil and Environmental Engineering, University of Technology Sydney, Ultimo, NSW 2007, Australia; Email: Cholachat.Rujikiatkamjorn@uts.edu.au

[d]Senior lecturer, Transport Research Centre, School of Civil and Environmental Engineering, University of Technology Sydney, Ultimo, Australia; Email: Trung.Ngo@uts.edu.au

Abstract

The most common railway ballast is produced by quarrying, and its mechanical characteristics are crucial for both stability and drainage for safer and faster rail operations. Ballasted tracks have certain drawbacks, primarily because ballast starts to degrade over time. In this regard, reducing the rate of ballast degradation is vital to enhance track longevity and minimise maintenance costs. This paper demonstrates how segments of huge waste rubber tyres (e.g. 3m in diameter) from the mining industry can be used to improve stability of tracks, while contributing to reduced ballast deformation and degradation. By placing arched segments cut from these tyres along the track shoulders beyond the edge of sleepers (i.e. the plan view gives a schematic impression of a caterpillar), the in-situ lateral confining pressure can be increased

from 20-25 kPa (standard track) to 40-50 kPa. This novel idea of *Confined-Caterpillar Track* (CCT) was tested at a prototype physical model (1:1 scale) at the National Facility for the Heavy-haul Railroad Testing (NFHRT), and the experimental outcomes compared to the performance of a conventional track. Apart from constributing to at least 25% saving of quarried aggregates, the test results prove that the CCT concept can curtail the lateral displacement and settlement of the ballast layer, while reducing particle breakage and effecting significant stress reduction in the underlying substructure layers.

3

1. Introduction

Australia generates more than 50 million waste rubber tyres annually, and the lack of effective recycling techniques and irregular dumping often lead to massive stockpiles with grave environmental concerns. In particular, large off-the-road (OTR) tyres discarded by the mining industry (diameter > 3 meters and weight > 3 tonnes) are the most challenging from a disposal point of view, hence the need for innovative solutions to reuse them on a large scale. This study promotes an innovative adoption of using these tyres to improve the stability of ballasted rail tracks, where arch segments can provide additional confinement at the track shoulders and curtail lateral displacement of ballast. Given the extensive heavy-haul track network in Australia (over 35,000 km), large-scale utilisation of OTR tyres can offer a significant technological innovation as well as a sustainable environmental option embracing a circular economy perspective.

As a result of increasing train speeds and axle loads in recent times (Connolly *et al.* 2020), more intense cyclic loading is inevitably transmitted to the track components. Consequently, this can cause excessive ballast deformation and degradation, thus affecting the track's instability and significantly increasing the cost of track maintenance (Li and Selig, 1998). Nimbalkar and Indraratna (2016) demonstrated that insufficient in-situ confining pressure leads to the loss of lateral stability of ballast while causing significant particle breakage, which was extensively examined through large-scale process simulation testing by Lackenby et al. (2007). A conventional track has shoulder ballast (usually elevated to a mound) to provide some confinement to the ballast. Typical in-situ confining pressure varies in the range of 15-30 kPa (Biabani *et al.* 2016), whereas several laboratory studies showed that the optimum confining pressure for a typical 300mm thick ballast layer should be in the range of 35-70 kPa (Indraratna *et al.* 2005; Lackenby *et al.* 2007).

The role of confining pressure on the shear strength and deformation behaviour of various types of rockfill was extensively studied. By varying the confining pressure widely from 1 kPa to about 250 kPa, Charles and Watts (1980), Marachi *et al.* (1972) and Indraratna *et al.* (1998) reported that the internal friction angle and dilation characteristics of the granular mass would be significantly governed by the magnitude of confining pressure. In real-life situations where the ballast layer is relatively thin, the confining pressure within the layer is often very low, and highly angular aggregates experience significant dilation and associated breakage upon loading. Lackenby *et al.* (2007) found that under increased confining pressure (σ_3), dilation of ballast is suppressed, and the primary degradation mechanism also changes from the breakage of angular corners to splitting across the body of particles. Indraratna *et al.* (2005) proposed three zones of particle degradation concerning confining pressure, namely: (a) dilatant, unstable degradation zone (*DUDZ*, $\sigma_3 < 30$ kPa), (b) optimum degradation zone (*ODZ*, $30 < \sigma_3 < 75$ kPa) and (c) compressive, stable degradation zone (*CSDZ*, $\sigma_3 > 75$ kPa). The recommended values of these zones are summarised in Table 1 based on maximum cyclic deviatoric stress. Based on large-scale cyclic triaxial tests (specimen diameter = 300 mm, height = 600 mm), Lackenby *et al.* (2007) reported a significant decrease in the axial strain as the confining pressure increased to about 50 kPa, beyond which only a marginal change was observed. They also reported the change in the volumetric behaviour of ballast (changing from dilative to compressive) with increased confinement. The reduction in dilation during shearing ensures a greater particle-to-particle contact in the ballast layer (more uniform internal stress distribution), thus reducing particle breakage. In view of the above, there is is no doubt that achieving optimum confinement in the track substructure is desirable for enhanced track longevity with lesser permanent settlements over its service life.

There are numerous methods to provide additional confinement to granular material, such as the use of geocell (Biabani *et al.* 2016; Leshchinsky and Ling, 2013; Liu *et al.* 2018; Tang

5

and Yang, 2013), lateral restraints, and winged sleepers (Indraratna *et al.* 2005; Lackenby *et al.* 2007) and geogrids (Esmaeili *et al.* 2017; Hussaini *et al.* 2016; Liu *et al.* 2016; Yu *et al.* 2019). Geogrids placed at the ballast-capping interface or inserted within the ballast layer are one of the standard practices for promoting efficient interlocking of particles through lateral restraint (Brown *et al.* 2007; Tutumluer *et al.* 2012). In order to provide adequate lateral stability to the track, the ballast shoulder can be altered beyond the edge of sleepers (Le Pen *et al.* 2014). However, the increase in in-situ confining pressure provided by these track shoulders is still relatively small (<25 kPa) (Harkness *et al.* 2016; Lackenby *et al.* 2007), so the additional use of quarried material to construct broader track shoulders is not always a feasible and economical option. Under repeated cyclic loading, low confining pressure is not sufficient to effectively control the excessive lateral displacement of aggregates (Powrie *et al.* 2007), leading to ballast degradation and excessive track settlement (Suiker *et al.* 2005). Particles that spread laterally, causing dilation of the granular assembly, can weaken the horizontal residual stresses, which lower the overall track stability and the ability to withstand increased axle loads (Waters and Selig, 1994). Indraratna et al. (2010) showed that optimising lateral confinement can contribute to substantial savings on track maintenance by extending the longevity of ballast.

2. Confined-Caterpillar Track (CCT)

Figure 1(a) shows the cross-section of a giant OTR tyre where each tyre has a diameter of about 3400 mm and a tread width of about 1160 mm. Since the total thickness of the standard ballast layer for heavy-haul railways in Australia is typically about 550 mm (i.e. 300 mm load-bearing ballast and 250 mm crib ballast), the tyre was first cut along the centre of the tread (as shown by the red dash line in Fig. 1a), followed by cutting the circular tyre with a particular central angle (60 degrees in this case) to obtain the "L" shaped segments, as shown in Fig. 1b. It can

be observed that the curved sidewall of the tyre (1000 mm long) prevents the segments from being ideally placed close to the sleepers, so the length of the sidewall was optimally cut to 300 mm (Figure 1b). A sidewall had to be cut into segments enabling the placement close to the sleepers. Figure 1(c) shows the standard dimensions of a heavy haul rail track, while Figure 1(d) shows the cross-section of the proposed solution. These elements are placed in such a way that the sidewall is in contact with the sub-ballast layer; the tread is placed upwards, resulting in a curved "*L*" shape at the edge of the track. As a result, the height of the segment (about 580 mm) becomes comparable with the standard ballast height, i.e., 550 mm. Considering the self-weight of each segment (around 250 kgs) plus the weight of ballast held within it (around 450 kgs), the Confined-Caterpillar Track (CCT) along the track shoulders is able to curtail the lateral movement of ballast aggregates. From the top view (Figure 1e), the assembly mimics the shape of a caterpillar and can be named as "*Confined-Caterpillar Track (CCT)*".

 It is noted that based on the one-to-one prototype testing of the CCT system without any tie or fixity, the outward lateral displacements of these tyre segments were less than 1 mm, which is negligible in relation to the scale of railway substructure. Hence, a tie/fixity may not be required to ensure their stability while in operation. In addition, it is evident that during the maintenance process, there might be the need to move or replace an individual segment, and therefore, having a rigid tie/fixity of the joints may not always be feasible. The off-the-road (OTR) tyres are manufactured to be used for massive trucks in mining industry where they are subjected to much harsher loading and climatic conditions and continual rotational movement than the relative static conditions encountered on the shoulders of a railway track. The robust construction of these extremely heavy-duty tyres with embedded steel bars and mesh, makes them ideal for exposure to ambient weather conditions. These rubber tyres are produced to take high heat and abrasion and to resist degradation under continual wet conditions and very high summer temperatures. Tyre supply companies have done much research to prove that any

breakdown of this heavy-duty rubber when not exposed to UV light will take over 150 years before any significant degradation can occur (Goryunov et al. 2019, Bridgestone, 2018).

3. Size and placement of tyre elements

In order to implement the CCT, it is imperative to determine the size of tyre segments and the placement location in relation to sleepers (i.e., shoulder width). The curved tyre segments were analysed using an open cylindrical shell theory to obtain an optimum segment of 60° central angle (see Appendix), resulting in a segment length in the longitudinal direction of about 1800 mm. A total of 12 tyre arch segments can effectively form a railway track 10.8m long. It is noted that each tyre segment weighed around 250 kgs, the factors of safety (FoS) against sliding and overturning can be calculated by considering all the forces acting on the segment during the passage of a train. For the given test setting up in this study, the FoS against sliding and overturning were determined to be 1.28 and 1.43, respectively.

Based on extensive large-scale laboratory testing and field measurement, Indraratna and Ngo (2018) reported that the vertical stresses at the ballast-sleeper interface varied between 150-350 kPa for axle loads of 20 to 35 tonnes and speeds of 40 to 120 km/hr. These stress values were adopted in this study to calculate the predicted lateral stress generated in the ballast layer. Figure 2 shows the calculated lateral earth pressures using the Rankine's earth pressure theory for both at-rest and active conditions based on the vertical stresses at the ballast-sleeper interface, for a friction angle of ballast of 50°. The value of 50 degrees is common for the apparent friction angle of highly angular fresh latite basalt used as railways ballast at relatively constant volumetric strain, i.e., approaching a critical state after 20% of axial strain in large-scale triaxial testing (Indraratna et al. 2011). Due to the rigidity and the weight of tyre segments, it is assumed that CCT provides a flexible non-displacement boundary on the sides of the track. When the at-rest condition is maintained, the optimum range of confining pressure (40-70 kPa) to minimise ballast degradation can also be achieved, as suggested by Lackenby et al. (2007).

In terms of shoulder width, a minimum width of 200mm from the end of the sleepers is required to allow maintenance and tamping activity. A shoulder width greater than 400 mm can result in an excessive amount of quarried ballast. In this study, a distance of 300 mm from the end of the sleepers was chosen. In comparison to conventional track, 25% savings of quarried aggregates can be obtained.

The clearance between sleepers and tyre segments was influenced by the current maintenance requirements, including the minimum clearance for machinery movement during track maintenance. If placed too far from the sleepers (say beyond 450 mm), there will be no material saving and no considerable effect on the performance of tracks. In the current project, after discussing with the industry track engineers from Sydney Trains (c/o Transport for New South Wales) and Rio Tinto Pty. Ltd., it was agreed that a clearance in the range of 200 to 400 mm between the sleepers and the tyre segments would be acceptable for effective track confinement. However, there was no numerical (sensitivity) analysis conducted to establish this optimal clearance range, and this is a limitation of the current study. It is noted that the height of the tyre segments is around 550 mm, which is comparable to a standard thickness of ballast (300 mm load-bearing ballast + 250 mm shoulder ballast) in a railway track. In addition, the thickness of the tyre wall is around 75-90mm (with strong interior reinforced steel bars), which prevents the tyre elements from becoming prone to tilting or outward squeeze.

4. Physical modelling of CCT

Considering the dimensions of CCT, it was impossible to incorporate a CCT in the prismoidal triaxial chamber (Jayasuriya *et al.* 2019; Navaratnarajah and Indraratna, 2017). Therefore, the state-of-the-art National High-speed Facility of Rail Testing (NHFRT), established by the second author in 2017 in Russel Vale (near Wollongong City), was adopted to simulate a full-scale (1:1) physical model of CCT. It comprised a test pit, loading frame, hydraulic loading

system including servo-mechanical devices, pumps and electrical layouts, an instrumentation and data acquisition system, and the overhead bulk handling setup. The cyclic loading was applied through the four actuators acting in two pairs to simulate a maximum axle load of up to 40 tonnes at a maximum frequency of 35 Hz (i.e., a train speed up to 200 km/h). The loading with controlled amplitude and frequency was applied to the steel rails fixed on concrete sleepers (Indraratna *et al.* 2021).

4.1. Test setup for Confined Caterpillar Track

Figure 3 shows the cross-section of the conventional track and CCT, with an array of instrumentation. A total of twenty stainless-steel pressure cells (200 mm diameter) were installed at various locations (e.g., below the loading points of the dynamic actuators), to measure the transient vertical and horizontal stresses. The maximum measuring ranges of these pressure cells at the sleeper-ballast, ballast-capping and fill-subgrade interface were 2.5 MPa, 1 MPa and 500 kPa, respectively. They were chosen based on the previous laboratory and field tests (Esmaeili et al. 2017; Indraratna et al. 2010; Maragakis et al. 2001; Nimbalkar and Indraratna, 2016). In order to measure the permanent settlements, a total of fourteen settlement pegs were installed at different depths in the structural fill, capping, and ballast layers during the construction process, with special care during tamping. In order to record the lateral movement of ballast under sleeper, a total of 3 customised horizontal extensometers (2.5m long) fitted with 100mm x 100mm x 10 mm end blocks with a range of 150 mm were installed together with protected stainless-steel casing. To measure the acceleration and vibration, two 600g triaxial accelerometers were mounted on the rail and sleeper using epoxy glue. As shown in Figure 3, at the bottom of the test pit, a 75-mm layer of coarse-grained gravel was placed as a drainage layer. This layer was then covered by a geotextile filter to prevent it from clogging. Using an excavator, a fine-grained subgrade was placed in the pit and compacted with a

vibrating plate to a thickness of about 800 mm in four layers to the desired dry unit weight of 16.5 kN/m^3 at a moisture content, w = 20%.

On top of the subgrade, a structural fill layer was placed up to 650 mm in thickness, having a moisture content of 11.5%. This layer was also compacted in sub-layers (150-200 mm) using a vibrating plate in order to achieve a desired dry unit weight of 18.5 kN/m^3. The structural fill was followed by the placement of a 180 mm thick capping layer (sub-ballast) comprising a sand and gravel mixture. This capping layer was compacted in two 90-mm thick sub-layers to a dry unit weight of 19.5 kN/m^3, equivalent to approximately 90% of the maximum dry density based on the standard Proctor compaction method in accordance with AS 1289.5.1.1 (2017). Sand cone tests were carried out in accordance with ASTM D1556 (2016) to ensure the target unit weight. Figure 4 shows the particle size gradation curves of the materials of the track substructure. Latite basalt aggregates used as ballast were sourced from a quarry south of Sydney. Ballast layer of 300mm in thickness was compacted using a plate vibrator in three 100-mm sublayers to achieve a unit weight of 16 kN/m^3. In the case of CCT section, four cut tyre segments were instrumented with strain gauges, as shown in Figure 5. The locations of actuators were referred to as north-west, south-east, etc.

Figure 6 shows the process of construction of CCT. Figure 6(a) shows the sand replacement method to measure the degree of compaction of the capping layer. After placing the four tyre segments at the desired locations on top of the capping layer, ballast was placed and compacted (Figs. 6(b) and 6(c)), followed by the placement of the rail-sleeper assembly (Fig. 6(d)). This track assembly had 6 concrete sleepers placed at a centre-to-centre distance of 600 mm, fastened to the steel rail using fasteners. Finally, the crib and shoulder ballast were compacted using a hand-held vibrating plate (Fig. 6(e)). Subsequently, the actuators suspended from the loading frame assembly could be conveniently hoisted to position using the overhead crane (Fig. 6(f)). Two steel walls were installed on two longitudinal ends of the track section to

prevent any movement of ballast in that direction and ensure a plane-strain condition. After completion of the test for conventional/unreinforced track, the ballast and capping layers were removed and replaced with fresh materials, however, the fill and subgrade layers in the pit were left undisturbed.

4.2. Loading program

The current study focuses on typical 25-tonne freight trains. As a result, the maximum load from each actuator was 12.5 tonnes (125 kN) to represent each wheel load. It was found that a minimum of 15 kN seating load was necessary to ensure proper contact between the rail and actuator tips as shown in Figure 7. The gradual increase to a mean load of 70 kN was achieved with a relatively slow loading rate followed by a sinusoidal loading frequency of 15 Hz over 500,000 cycles. The applied frequency of 15 Hz corresponds to the typical heavy-haul train speed of 60-80 km/h operating in most parts of Australia (Indraratna et al. 2011). It is worth mentioning that in the 1:1 scale testing, the loading occurs within the centreline of the tyre arcs, while in real-life tracks, the loading would occur in proximity to the joints between the tyre segments. However, as the self-weight of each segment (250 kgs) plus the weight of ballast held within it (around 450 kgs) offers substantial normal stress to resist sliding, these CCT tyre segments placed along the track shoulders are capable of curtailing the lateral movement of ballast and will not require any additional tie or fixity.

5. Test Results and Discussion

5.1. Vertical settlement

The vertical settlement of CCT during the application of cyclic loading in the NHFRT is shown in Figure 8. Compared to a conventional track tested in the NHFRT, the track with CCT achieves a stable state more quickly, i.e., at N= 50,000 cycles, whereas the conventional track shows increasing settlement even after 500,000 cycles. The behaviour of track with CCT is

similar to a smaller track section tested earlier by Indraratna et al. (2013), but shows a significantly smaller settlement with N. It is noted that the experiment reported by Indraratna et al. (2013) was conducted using a process simulation apparatus for a representative single sleeper track segment (800mm x 600mm x 600mm) which is different in dimensions to the much larger multi-sleeper physical model (1:1 scale) adopted in the current study. However, the scale of materials tested (ballast, capping and subgrade) and loading program are indeed very similar for both studies, and this makes the comparison relevant. Test results of CCT show the smallest settlement upon cyclic loading compared to all other plots, including real-life (Bulli) measurements, convincingly suggest the role of confining pressure provided by the rubber tyre segments in the CCT section, as further elaborated below. Comparing the final settlement after N=500,000 cycles, the CCT track shows a settlement of 9.85 mm as compared to 16.6 mm reported for a conventional track, i.e., a reduction of about 40%. When compared to the results obtained from Bulli track and data obtained from laboratory cubical triaxial tests (Indraratna *et al.* 2013), similar observations can be made where an initial rapid settlement occurs up to N=100,000 cycles, followed by gradually increasing settlement within N=300,000, and then remaining relatively constant to the end (N=500,000). In a practical sense, these measurements suggest that if we consider a newly constructed track, it is recommended to reduce the speed of trains during the early period of operation, where initial settlement can be rapid. As proven by Figure 8, a newly constructed track achieves almost 60% of its permanent settlement within N=50,000 cycles. As the CCT offers quicker shakedown to a stable foundation, a newly constructed CCT can be particularly beneficial for heavy-haul trains. It is noteworthy that the Russel Vale model track was purposefully built to mimic similar soil stratification and track substructure conditions of typical heavy haul tracks constructed in the south coast of New South Wales (i.e., south of Sydney). A field trial was conducted on a fully-instrumented track in the coastal town of Bulli (70km south of Sydney) to examine the

performance of fresh ballast versus recycled ballast and the role of artificial inclusions (Indraratna et al. 2010). It was constructed with latite basalt aggregates used for load-bearing ballast, overlying a conventional capping layer (compacted sandy gravel) and soft subgrade (clayey sand with some gravel), which had a very close resemblance to the substructure conditions tested in this study. The total thickness of the track bed was 450 mm, including a 300 mm ballast layer and a 150 mm capping layer. The train loading applied in the Bulli track was a 25-tonne axle load traveling at a speed of 60-80 km/h, which was also similar to the loading conditions applied in this study.

5.2. Lateral movement

Upon repeated loading in the absence of sufficient confinement, ballast moves laterally outwards from the centre of the track. This lateral movement causing dilation of the granular assembly reduces the particle-to-particle contact and decreases the load-bearing capacity of the ballast layer. Figure 9 shows the lateral movements of ballast measured at the edge of a sleeper under cyclic loading in comparison to that measured for a conventional track. It is seen that the CCT track achieves a stable lateral displacement very quickly at around 50,000 cycles, beyond which there is insignificant movement even when approaching 500,000 loading cycles. The CCT reduces the ultimate movement by about 40% (i.e., 9.09mm for the conventional track in contrast to 5.48mm for CCT), and prevents any further lateral spreading after the track achieves a stable shakedown level. In Fig. 9, comparing the CCT results to the field test data obtained from Bulli track and large-scale laboratory data (i.e. prismoidal process simulation triaxial chamber), there is no doubt that the CCT effectively and swiftly curtails lateral spreading of ballast.

5.3. Stress distribution along the depth

Figure 10(a) presents the distribution of vertical stress measured at different depths in the track after 100,000 cycles. Compared to the conventional track (i.e., no tyre segments), the CCT shows a reduced stress distribution with depth. For instance, at N=100,000 cycles, the vertical stresses on top of capping, fill and subgrade layers for a conventional track are 125, 110 and 95 kPa, respectively; in contrast, for the CCT the corresponding values are 98, 67 and 47 kPa, respectively. This demonstrates 21%, 39% and almost 50% reduction in the vertical stresses propagated to the underlying substructure layers, respectively. Moreover, the CCT track shows a substantial stress reduction at the bottom of the ballast layer compared to the conventional track. For instance, in a conventional track, the stress reduces by about 35% within the ballast layer, however, for a CCT, this reduction is as much as 53%. The measurements verify that the vertical stress is predominantly taken by the ballast assembly, which in turn favourably results in significantly reduced stress distribution transferred to the underlying substructures. CCT improves the particle-to-particle contacts attributed to the additional confinement.

Figure 10(b) shows the typical cyclic deviator stress measurements for different substructure layers during the testing of CCT, where the reduction in peak stresses with depth can be clearly observed. The CCT system reduces the transfer of vertical stress to the underlying capping and subgrade layers mainly attributed to the additional side confinement to the ballast provided by the CCT that reduces both the lateral movement and the axial displacement (settlement). This decreased ballast dilation has the equivalent outcome of increasing the apparent friction (particle interlock) and the effective stiffness of the ballast layer (Lackenby et al. 2007). This means that the ballast layer can then bear the bulk of the applied stress, resulting in less stress propagating to the underlying capping and soft subgrade layers. While the stress at the sleeper-ballast interface is higher for CCT than for conventional tracks, it decreases significantly with depth. At the ballast-capping interface, the stress measured for CCT is much less than that of a conventional track. For instance, the vertical stress measured for CCT is about 98 kPa,

compared to 126 kPa for a conventional track. It can be concluded that apart from curtailing lateral movement, the CCT offers a sustainable solution to reduce stress transfer to an underlying soft (and often saturated) subgrade and thereby considerably alleviate the chances of undrained yielding or failure.

5.4. Lateral stress developed in the ballast

Figure 11(a) shows the lateral stresses in the conventional and CCT track sections measured at N=50,000 cycles in the NHFRT plotted for 1 second. It is observed that the average lateral stress measured in CCT section is approximately 40 kPa, whereas this value is around 22.5 kPa for the conventional section. The increase in lateral stress is clearly attributed to the additional lateral confinement provided by the tyre segments. Figure 11(b) confirms that the maximum lateral movement at the top of tyre segments was less than 1 mm. In the absence of the tyre elements in a conventional track with the lateral spreading of ballast, the mobilised lateral stress of the conventional section is quite close to the active condition, whereas, the lateral stress of CCT section is in between the active and at-rest condition as a result of the restricted movement. The difference between the at-rest earth pressure and the observed lateral stress can be attributed to the flexibility of the tyre segments. The increased lateral stress also helps reduce the ballast layer's peak vertical stress. For instance, for the conventional track, the average vertical stress in the ballast layer is about 158 kPa, based on the average stress at the top and the bottom of the ballast layer. Assuming the condition of the plane strain and with an average lateral stress of 22.5 kPa, the deviatoric stress amounts to about 135 kPa. In contrast, for the CCT a similar calculation reveals a deviatoric stress of 114 kPa. This reduction of about 15% in the deviatoric stress can reduce ballast breakage, which is elaborated on below.

5.5. *Ballast Breakage*

After the completion of 500,000 cycles of loading, ballast aggregates were collected at different locations (e.g., below the sleeper and from the shoulder) to measure the breakage. The method proposed to quantify breakage by Indraratna et al. (2005) was adopted, in which the Ballast Breakage Index (BBI) considers the area subtended by the shift in the particle size distribution (PSD) curve (i.e. before and after testing), quantifying the area between the original PSD and the arbitrary line representing crushed ballast (i.e., smallest grain size of 2.36 mm for the starting boundary of coarse sand). Figure 12 shows typical particle size distribution curves for ballast samples before and after testing, and the measured BBIs are given in Table 2. The BBIs below the north-west and south-east actuators are 0.092 and 0.087, respectively. Not surprisingly, at the exact locations of the conventional track, Indraratna et al. (2021) reported significantly higher BBI values of 0.115 and 0.143, which demonstrate a reduction of 20% and 39%, respectively. Similarly, the BBIs of the crib and shoulder ballast in the CCT section were 0.069 and 0.051, respectively, whereas these values were 0.085 and 0.074 for the conventional track showing a reduction of 19% and 31%, respectively. Compared to the conventional track, the CCT section sustains an average BBI reduction of about 27%. This reduction in particle breakage can be attributed to the increased lateral confinement provided by tyre segments ensuring a better particle packing arrangement upon loading. In a practical sense, this improvement translates into enhanced track longevity and a reduction in track maintenance costs..

5.6. *Vibrations on rail and sleeper*

Figure 13 compares accelerations measured on the rail in the CCT section with those of the conventional track. It is observed that the inclusion of tyre elements decreases the vibrations by about 25%, i.e. peak acceleration reduces from about 7 m/s^2 (conventional track) to 5 m/s^2

(CCT track). It is noted that although the tyre elements have to be placed away from the sleeper edges to prevent interfering with track inspection and maintenance activities, its effect on decreasing rail vibrations is significant, and this is attributed to reduced particle movement within a well-interlocked ballast assembly.

In Australian tracks, hanging sleepers have contributed to significant vibrations. The main reason why the CCT system reduces rail vibrations compared to conventional tracks is its ability to prevent the lateral movement of ballast shoulders, which in turn, reduces the occurrence of hanging sleepers. When conventional tracks were tested recently in the south coast of NSW, the authors noted that excessive lateral displacement of ballast at a hanging sleeper caused undue vibrations. In a field trial in Western Sydney, the gap between the sleeper and the ballast layer resulting from this lateral ballast displacement significantly increased the acceleration measured on the rail.

6. Conclusions

This paper presented the experimental results of a full-scale physical model test conducted on the novel *Confined-Caterpillar Track* (CCT) subjected to a 25-tonne axle load applied at a frequency of 15 Hz over 500,000 loading cycles. This track was designed by replacing a part of the shoulder ballast with recycled rubber tyre segments to provide additional lateral confinement to the load-bearing ballast. The performance of CCT was compared to a standard track, considering ballast deformation, degradation and vibrations. Based on this study, the following conclusions could be drawn:

a) The CCT reduced the ultimate vertical settlement of the track after 500,000 cycles by about 40% (CCT showed a settlement of 9.85 mm as compared to 16.6 mm measured for a conventional track). When compared to the results obtained from field trials with similar axle loads and frequencies, similar reductions in the vertical settlement were observed. The CCT also achieved the shakedown phase quicker than a conventional

18

track (at 50,000 cycles compared to 100,000 cycles for a conventional track). Beyond the shakedown phase, CCT offers a much more stable track by reducing further settlements as compared to a conventional track.

b) When compared to a conventional track tested at the NHFRT, the CCT did not only reduce the ultimate lateral movement by about 40% (9.09mm for conventional track compared to 5.48mm for CCT), but also did not allow any further lateral spreading of ballast after achieving a state of shakedown.

c) The CCT could effectively reduce the stress transferred to the underlying substructure layers. For instance, at 100,000 load cycles based on a typical 25-tonne axle load applied at a frequency of 15 Hz, there was a significant reduction of about 21%, 39% and 50% on the vertical stresses generated on top of capping, fill and subgrade layers, respectively. In a practical sense, a considerable reduction of the stress at a soft subgrade layer carries important implications in minimising undue yielding under heavy haul traffic.

d) For the CCT, the lateral stress in the ballast layer increased to about 42 kPa from about 22.5 kPa, corresponding to the conventional track. This additional lateral stress could be attributed to the presence of a non-yielding boundary that provided better in-situ confinement to the load-bearing ballast enabling it to achieve reduced dilation of the granular assembly, hence significantly diminished breakage.

e) The CCT track showed a significant reduction in ballast breakage compared to the conventional track under similar axle load amplitude and frequency. On average, a substantial reduction in particle breakage of about 27% was observed for the load-bearing ballast. In a practical sense, the reduced ballast breakage is improvement translates into enhanced track longevity and a reduction in track maintenance costs.

In essence, the outcomes of this study prove that the use of recycled tyre segments not only offers an attractive environmental solution for reduced quarrying and associated carbon emissions, but also provide a novel and sustainable track stabilisation technique for enhanced performance under cyclic loading, while extending the service life of ballasted tracks.

CRediT authorship contribution statement

Soumyaranjan Mishra: Formal analysis, Methodology, Investigation Writing –review and editing. **Buddhima Indraratna:** Conceptualisation, Methodology, Supervision, Writing – original draft, Writing – review and editing. **Cholachat Rujikiatkamjorn**: Supervision, Methodology, Writing – review and editing. **Trung Ngo**: Supervision, Writing – review and editing.

Declaration of Competing Interest

The authors declare that they have no known competing financial interests or personal relationships that could have appeared to influence the work reported in this paper.

Data Availability

Data generated or analyzed during this study are available from the corresponding author upon reasonable request.

Acknowledgment

University of Wollongong and the University of Technology Sydney for their assistance during

the experimental program amidst COVID-19 restrictions.

Appendix A

Figure A-1(a) shows a single unit of the confined-caterpillar structure with height (H), thickness (t) and central angle (2θ). It is assumed that the sides ($AA'D'D$ and $BB'C'C$) are simply supported. Figure A-1(b) shows the forces acting on an infinitesimal element of height dx and angle $d\theta$, located on the central plane of the element ($A''B''C''D''$). This element was analysed using theory of open cylindrical shells.

(a)

(b)

(c)
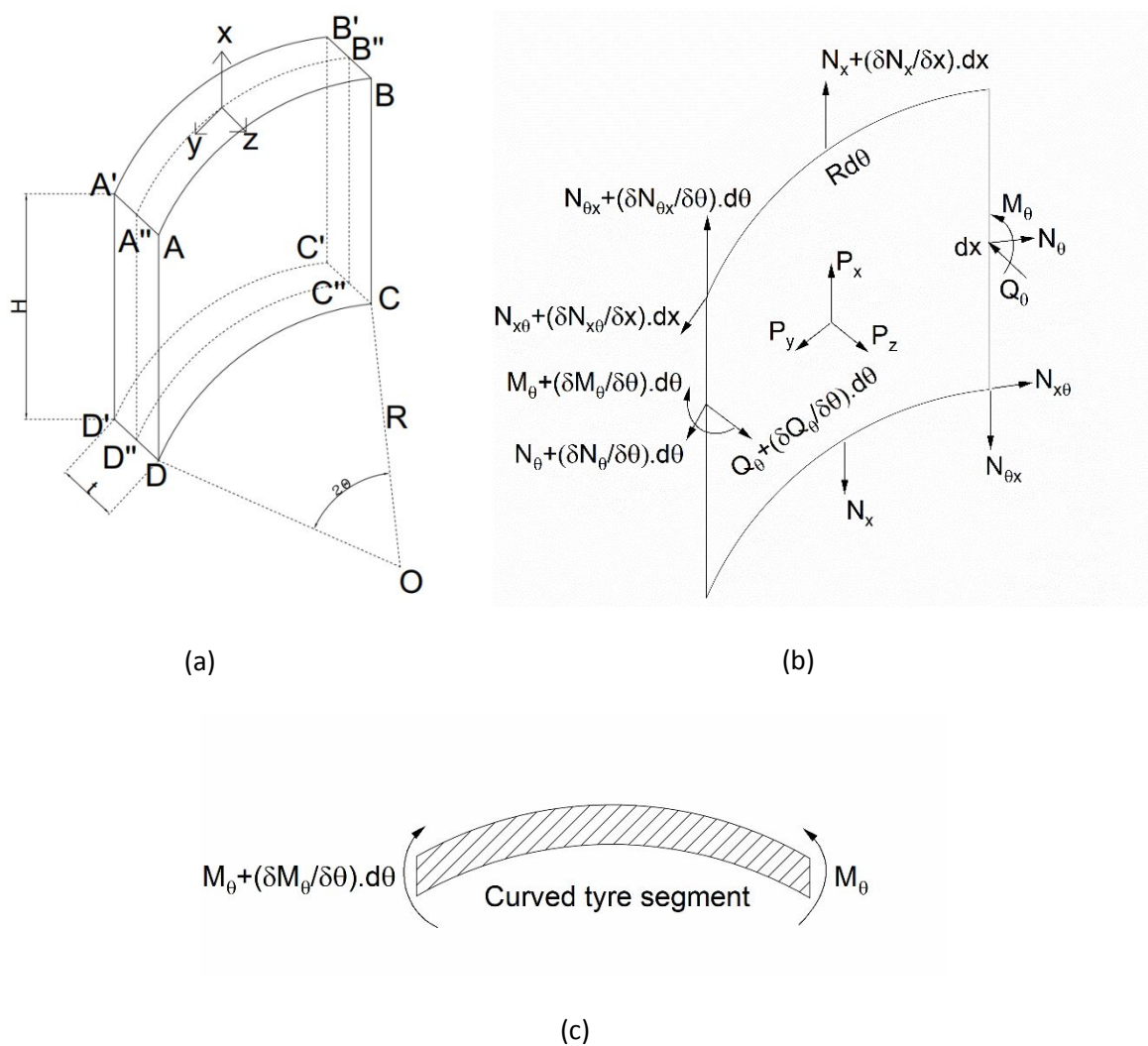
Figure A-1. (a) Single unit of CCT assumed as a thin shell; (b) Stress resultants in infinitesimal shell element on the central plane; and (c) Plan view of the segment with the moments

23

$dy = Rd\theta, N_x, N_\theta =$ body forces per unit length,

$P_x, P_y, P_z =$ external forces per unit area,

The assumptions in this derivation are as follows:

1.　The material is homogeneous, linear-elastic and isotropic.

2.　The bending resultants $M_x, M_{x\theta}, M_{\theta x}$ are insignificant as compared to M_θ, and may be ignored. That means that the primary direction of bending is considered across the face of the arched element.

3.　The movement of the element at both ends (i.e. *AA'D'D* and *BB'C'C* planes) are restricted across y-direction, which assumes zero displacements along the longitudinal direction of the track. Hence, $\varepsilon_2 = 0$ & $\varepsilon_{12} = 0$.

Now, applying force equilibrium in all three directions, the following equations are obtained.

$$\sum F_x = 0$$
$$\therefore \frac{\partial N_x}{\partial x} + \frac{\partial N_{\theta x}}{R\partial \theta} + P_x = 0 \quad (1)$$

$$\sum F_y = 0$$
$$\therefore \frac{\partial N_{x\theta}}{\partial x} + \frac{\partial N_\theta}{R\partial \theta} + P_y = 0 \quad (2)$$

$$\sum F_z = 0$$
$$\therefore \frac{\partial Q_\theta}{R\partial \theta} + \frac{N_\theta}{R} + P_z = 0 \quad (3)$$

Taking moments about x-axis,

$$\frac{\partial M_\theta}{R\partial \theta} - Q_\theta = 0 \quad (4)$$

Taking moments about z-axis,

$$N_{x\theta} = N_{\theta x} \;\; (5)$$

Eliminating Q_θ from equation (3) and (4),

$$\frac{\partial^2 M_\theta}{R^2 \partial \theta^2} + \frac{N_\theta}{R} + P_z = 0 \;\; (6)$$

Eliminating $N_{\theta x} \,\&\, N_{x\theta}$ using equation (1), (2) and (5),

$$\frac{\partial^2 N_x}{\partial x^2} - \frac{\partial^2 N_\theta}{R^2 \partial \theta^2} + \frac{\partial P_x}{\partial x} + \frac{\partial P_y}{R \partial \theta} = 0 \;\; (7)$$

Finally, eliminating N_θ from Equation (6) and (7),

$$\frac{\partial^4 M_\theta}{R^4 \partial \theta^4} + \frac{1}{R}\frac{\partial^2 N_x}{\partial x^2} + \frac{1}{R}\left(\frac{\partial P_x}{\partial x} - \frac{\partial P_y}{R \partial \theta} \right) + \frac{\partial^2 P_z}{R^2 \partial \theta^2} = 0 \;\; (8)$$

The loads P_x, P_y, P_z were assumed to be uniformly distributed loads, and hence their spatial derivatives are zero. Equation (8) was solved using the methods described by Gibson and Neal (1965), which yields the variation of body force as shown in Fig. A-2, for an applied stress of 30, 45 and 60 kPa. These values were chosen based on the optimum confining pressure zones as suggested by (Lackenby *et al.* 2007). A central angle of 60° was chosen for this particular case. It is noted that, for this case, the bending action (theta) was much more dominant than the membrane action (x-direction) because the tyre segments are cut; therefore, Figure A-2 shows only the body force generated along that direction and not in the x-direction.
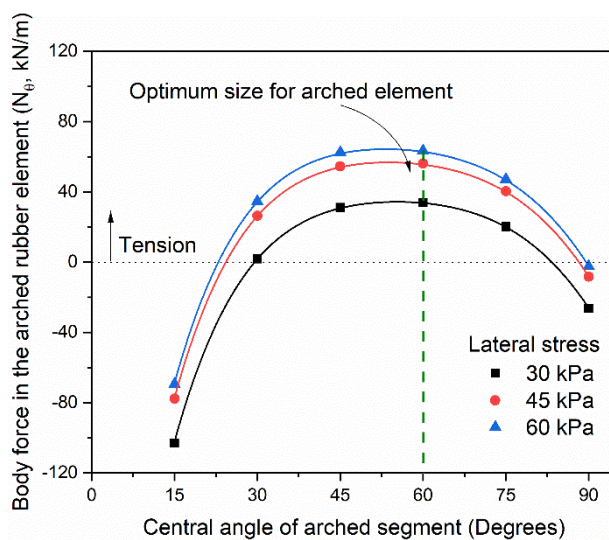
Figure A-2. Varitation of body force in the curved tyre element for different central angle

References

ASTM. (2016). Standard Test Method for Density and Unit Weight of Soil in Place by Sand-Cone Method. In *D1556*: American Society of Testing and Materials.

Biabani, M. M., Ngo, N. T., and Indraratna, B. (2016). Performance evaluation of railway subballast stabilised with geocell based on pull-out testing. *Geotextiles and Geomembranes, 44*(4), 579-591. doi:10.1016/j.geotexmem.2016.03.006

Bridgestone 2018. https://www.bridgestone.com/products/diversified/conveyorbelt/advanced_compounds/heat_resistant.html (accessed 21 June 2022)

Brown, S. F., Kwan, J., and Thom, N. H. (2007). Identifying the key parameters that influence geogrid reinforcement of railway ballast. *Geotextiles and Geomembranes, 25*(6), 326-335. doi:10.1016/j.geotexmem.2007.06.003

Connolly, D. P., Dong, K., Alves Costa, P., Soares, P., and Woodward, P. K. (2020). High speed railway ground dynamics: a multi-model analysis. *International journal of rail transportation (Online), 8*(4), 324-346. doi:10.1080/23248378.2020.1712267

Esmaeili, M., Zakeri, J. A., and Babaei, M. (2017). Laboratory and field investigation of the effect of geogrid-reinforced ballast on railway track lateral resistance. *Geotextiles and Geomembranes, 45*(2), 23-33. doi:10.1016/j.geotexmem.2016.11.003

Gibson, J. E., and Neal, B. G. (1965). *Linear Elastic Theory of Thin Shells*: Elsevier Ltd.

Goryunov, S., Khoreshok, A., Grigoryeva, N., Alitkina, O. (2019). The research of operational temperatures of dump trucks tires. The First Interregional Conference Sustainable Development of Eurasian Mining Regions, DOI: 10.1051/e3sconf/201913401014

27

Harkness, J., Zervos, A., Le Pen, L., Aingaran, S., and Powrie, W. (2016). Discrete element simulation of railway ballast: modelling cell pressure effects in triaxial tests. *Granular Matter, 18*(3). doi:10.1007/s10035-016-0660-y

Hussaini, S. K. K., Indraratna, B., and Vinod, J. S. (2016). A laboratory investigation to assess the functioning of railway ballast with and without geogrids. *Transportation Geotechnics, 6*, 45-54. doi:10.1016/j.trgeo.2016.02.001

Indraratna, B., Ionescu, D., and Christie, H. D. (1998). Shear behaviour of railway ballast based on large-scale triaxial tests. *Journal of Geotechnical and Geoenvironmental Engineering, ASCE, 124*(5), 434-449.

Indraratna, B., Lackenby, J., and Christie, D. (2005). Effect of confining pressure on the degradation of ballast under cyclic loading. *Géotechnique, 55*(4), 325-328.

Indraratna, B., Nimbalkar, S., Christie, D., Rujikiatkamjorn, C. and Vinod, J. S. (2010). Field assessment of the performance of a ballasted rail track with and without geosynthetics. Journal of Geotechnical and Geoenvironmental Engineering,136(7): 907–917.

Indraratna, B., and Ngo, N., T. (2018). *Ballast Railroad Design: SMART-UOW Approach*: CRC Press.

Indraratna, B., Ngo, N. T., and Rujikiatkamjorn, C. (2013). Deformation of Coal Fouled Ballast Stabilized with Geogrid under Cyclic Load. *Journal of Geotechnical and Geoenvironmental Engineering, 139*(8), 1275-1289. doi:10.1061/(asce)gt.1943-5606.0000864

Indraratna, B., Ngo, T., Ferreira, F. B., Rujikiatkamjorn, C., and Tucho, A. (2021). Large-scale testing facility for heavy haul track. *Transportation Geotechnics, 28*. doi:10.1016/j.trgeo.2021.100517

Indraratna, B., Salim, W., and Rujikiatkamjorn, C. (2011). *Advanced Rail Geotechnology - Ballasted Track*. London ;: CRC Press.

Jayasuriya, C., Indraratna, B., and Ngoc Ngo, T. (2019). Experimental study to examine the role of under sleeper pads for improved performance of ballast under cyclic loading. *Transportation Geotechnics, 19*, 61-73. doi:10.1016/j.trgeo.2019.01.005

Lackenby, J., Indraratna, B., McDowell, G., and Christie, D. (2007). Effect of confining pressure on ballast degradation and deformation under cyclic triaxial loading. *Géotechnique, 57*(6), 527-536. doi:10.1680/geot.2007.57.6.527

Le Pen, L., Bhandari, A. R., and Powrie, W. (2014). Sleeper End Resistance of Ballasted Railway Tracks. *Journal of Geotechnical and Geoenvironmental Engineering, 140*(5). doi:10.1061/(asce)gt.1943-5606.0001088

Leshchinsky, B., and Ling, H. (2013). Effects of Geocell Confinement on Strength and Deformation Behavior of Gravel. *Journal of Geotechnical and Geoenvironmental Engineering, 139*(2), 340-352. doi:10.1061/(asce)gt.1943-5606.0000757

Li, D., and Selig, E. T. (1998). Method for railroad track foundation design I: Development. *Journal of Geotechnical and Geoenvironmental Engineering, 124*(4), 316-322.

Liu, S., Huang, H., Qiu, T., and Kwon, J. (2016). Effect of geogrid on railroad ballast particle movement. *Transportation Geotechnics, 9*, 110-122. doi:10.1016/j.trgeo.2016.08.003

Liu, Y., Deng, A., and Jaksa, M. (2018). Three-dimensional modeling of geocell-reinforced straight and curved ballast embankments. *Computers and Geotechnics, 102*, 53-65. doi:10.1016/j.compgeo.2018.05.011

Navaratnarajah, S. K., and Indraratna, B. (2017). Use of Rubber Mats to Improve the Deformation and Degradation Behavior of Rail Ballast under Cyclic Loading. *Journal of Geotechnical and Geoenvironmental Engineering, 143*(6). doi:10.1061/(asce)gt.1943-5606.0001669

Nimbalkar, S., and Indraratna, B. (2016). Field Assessment of Ballasted Railroads Using Geosynthetics and Shock Mats. *Procedia Engineering, 143*, 1485-1494. doi:10.1016/j.proeng.2016.06.175

Powrie, W., Yang, L. A., and Clayton, C. R. I. (2007). Stress changes in the ground below ballasted railway track during train passage. *Proceedings of the Institution of Mechanical Engineers. Part F, Journal of rail and rapid transit, 221*(2), 247-262. doi:10.1243/0954409JRRT95

Standards Australia. (2017). In *AS 1289.5.1.1 Methods of testing soils for engineering purposes Soil compaction and density tests*: SAI Global (https://infostore.saiglobal.com/en-au/).

Suiker, A. S. J., Selig, E. T., and Frenkel, R. (2005). Static and Cyclic Triaxial Testing of Ballast and Subballast. *Journal of Geotechnical and Geoenvironmental Engineering, 131*(6), 771-782. doi:10.1061/(ASCE)1090-0241(2005)131:6(771)

Tang, X., and Yang, M. (2013). Investigation of Flexural Behavior of Geocell Reinforcement Using Three-Layered Beam Model Testing. *Geotechnical and Geological Engineering, 31*(2), 753-765. doi:10.1007/s10706-013-9625-7

Tutumluer, E., Huang, H., and Bian, X. (2012). Geogrid-Aggregate Interlock Mechanism Investigated through Aggregate Imaging-Based Discrete Element Modeling Approach. *International Journal of Geomechanics, 12*(4), 391-398. doi:10.1061/(ASCE)GM.1943-5622.0000113

Waters, J. M., and Selig, E. (1994). *Track Geotechnology and Substructure Management*. London: Institution of Civil Engineers.

Yu, Z., Woodward, P. K., Laghrouche, O., and Connolly, D. P. (2019). True triaxial testing of geogrid for high speed railways. *Transportation Geotechnics, 20*. doi:10.1016/j.trgeo.2019.100247

Table 1. Zones of confining pressure based on maximum cyclic deviatoric stress (Lackenby *et al.* 2007)

$q_{max,cyc}$ (kPa)	DUDZ	ODZ	CSDZ
230	<15 kPa	15-60 kPa	>65 kPa
500	<25 kPa	25-95 kPa	>95 kPa
750	<50 kPa	50-140 kPa	>140 kPa

Table 2. Particle size gradation of ballast before and after test

Sieve Size (mm)	Percentage Passing (%)				
	Initial gradation before test	Ballast collected underneath NW actuator	Ballast collected underneath SE actuator	Ballast collected between two rails	Ballast collected from shoulder
63	100	100	100	100	100
53	95.7	96.2	96.6	95.8	95.9
37.5	62.3	64.1	63.2	63.8	63.4
26.5	26.5	28.8	28.5	28.7	28.1
19	13.8	15.8	15.3	15.1	14.8
13.2	6.4	6.5	6.8	6.9	6.6
9.5	0	1.1	1.3	0.9	0.2
4.75	0	0.2	0.5	0	0
2.36	0	0	0	0	0
Measured BBI		**0.092**	**0.087**	**0.069**	**0.051**

(a)

(b)

(c)

(d)

(e)
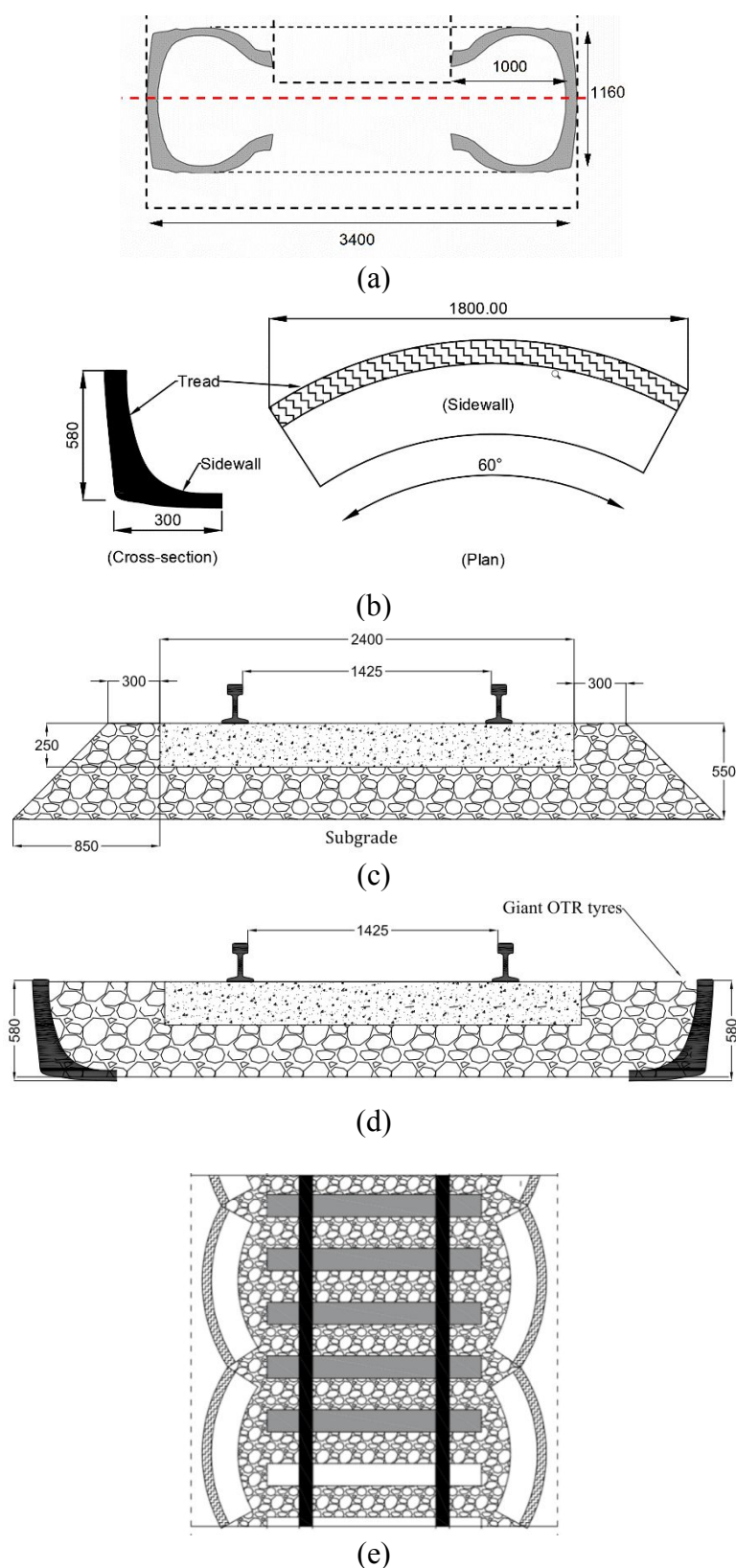
Figure 1. (a) Cross-section of the OTR tyre, (b) Cross-section and plan of the tyre

segments (c) Standard track dimensions for heavy-haul track, (d) vertical cross-section of the

confined-caterpillar track (CCT), and (e) Top view of CCT (All dimensions are in mm)

34
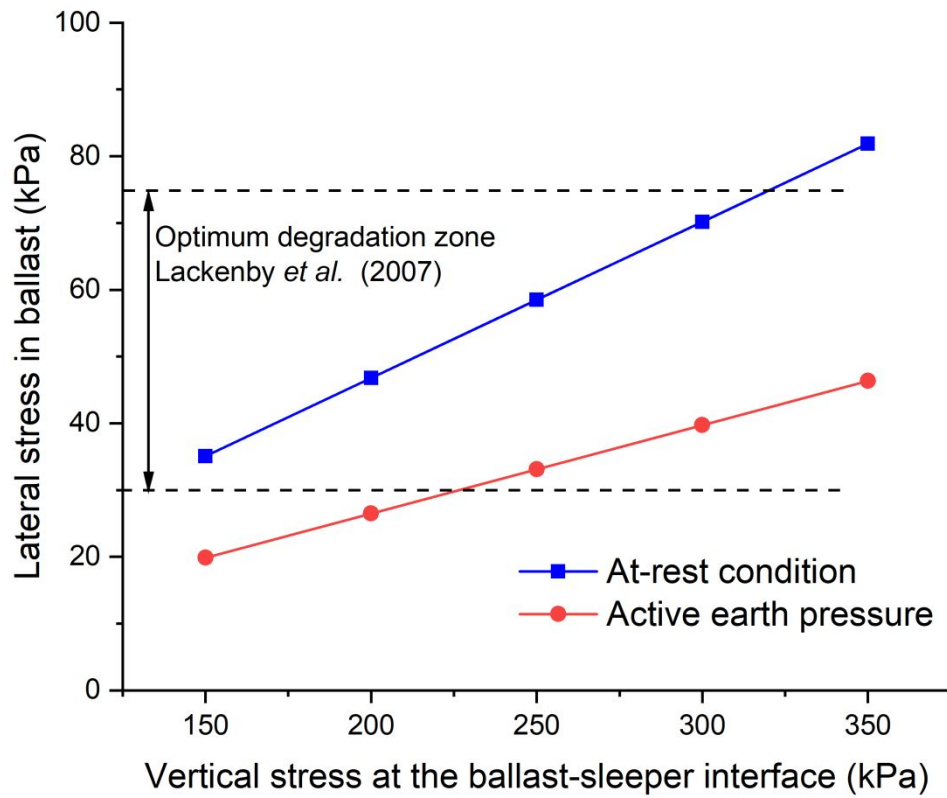
Figure 2. Calculated lateral stresses for different vertical stresses at the ballast-sleeper
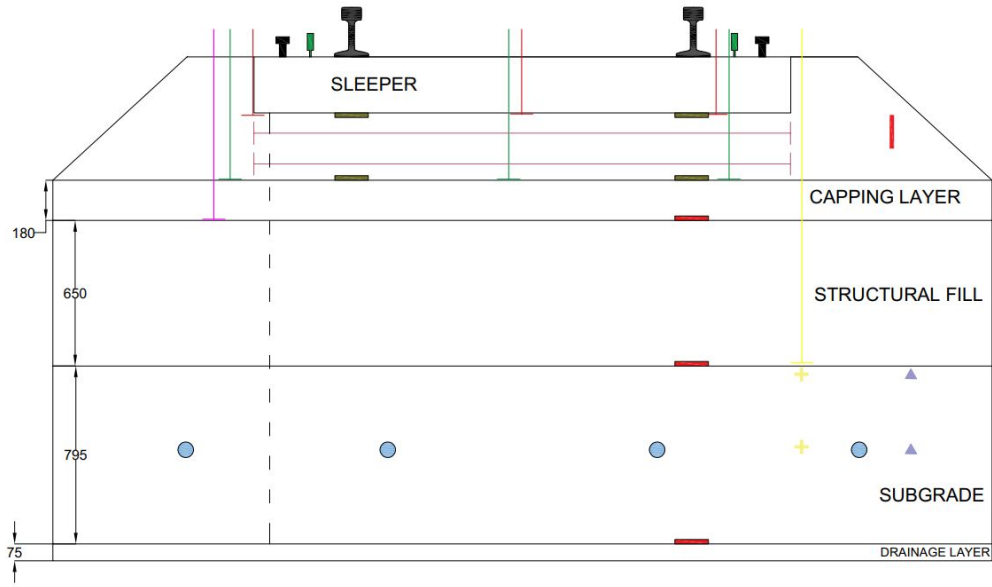
interface

(a)
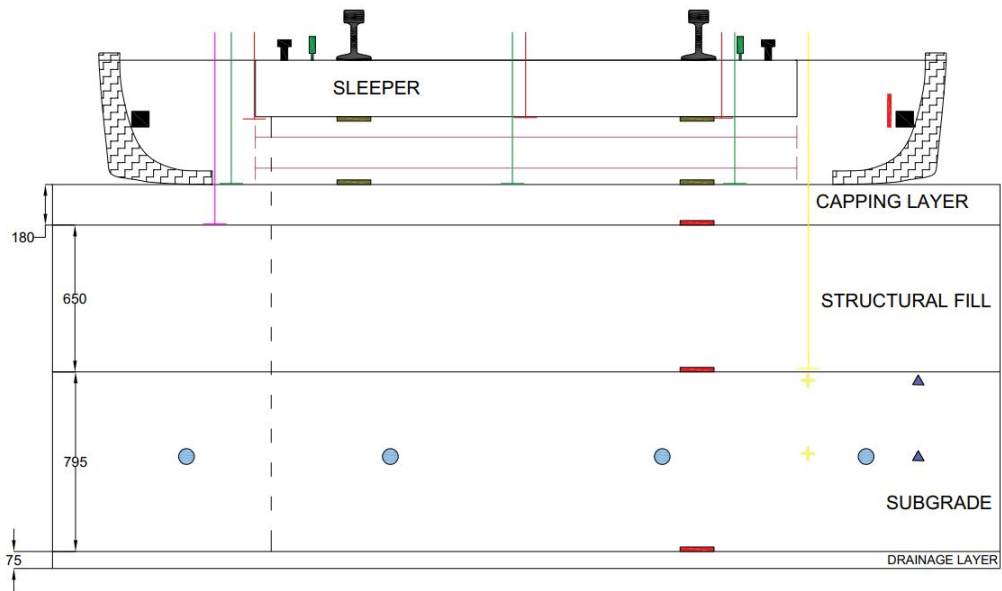
(b)

Figure 3. Cross-sectional view of: (a) conventional track and (b) *Confined-Caterpillar Track* (CCT) at the NHFRT (all dimensions are in mm)
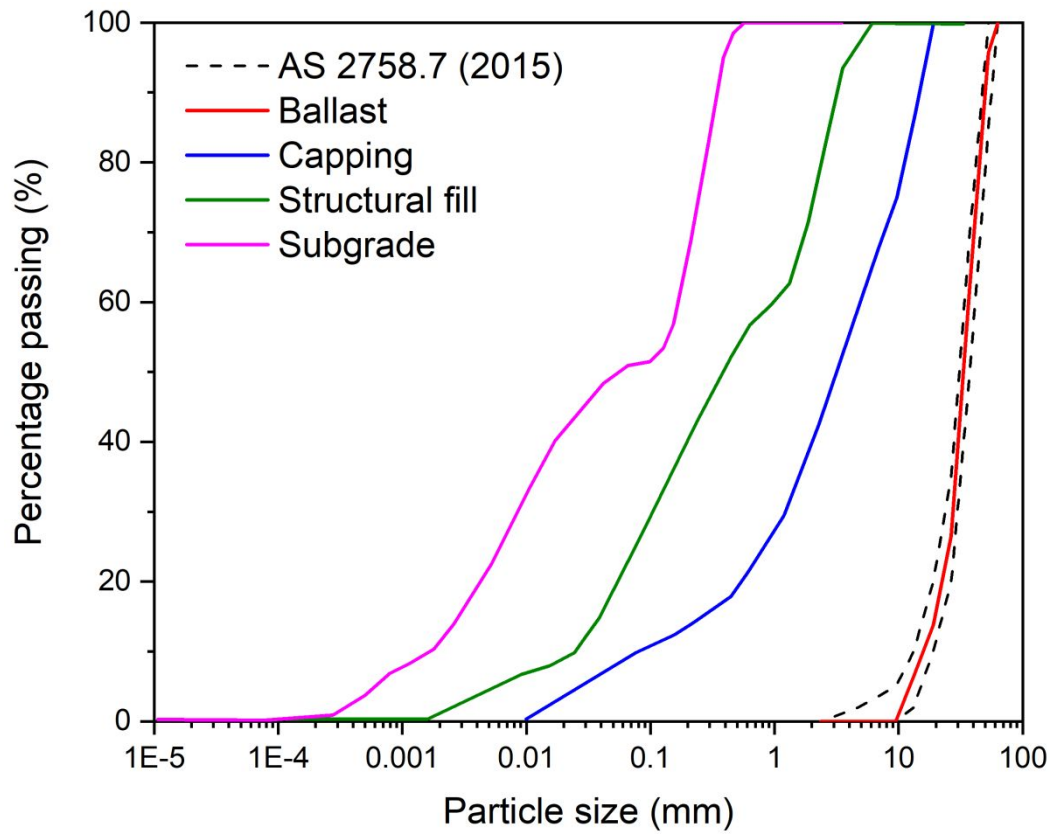
Figure 4. Particle size distributions of track substructure materials
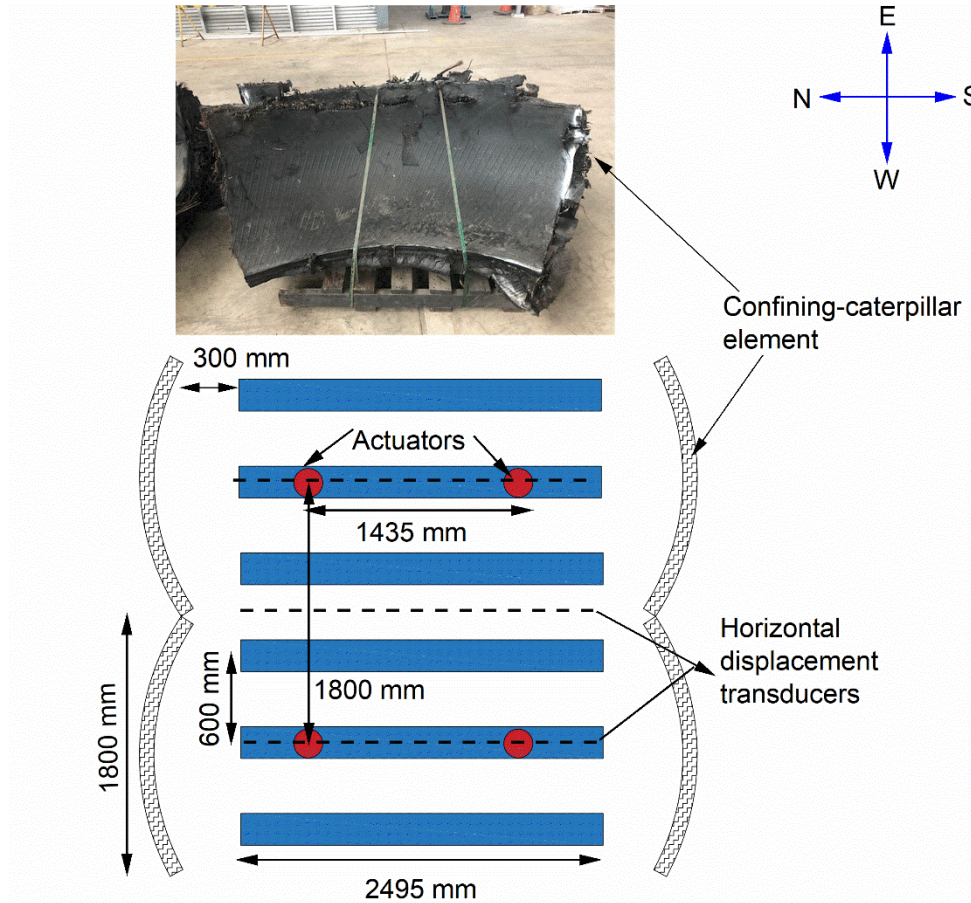
Figure 5. Plan view of the *Confined-Caterpillar Track* (CCT) at NFHRT

(a)

(b)
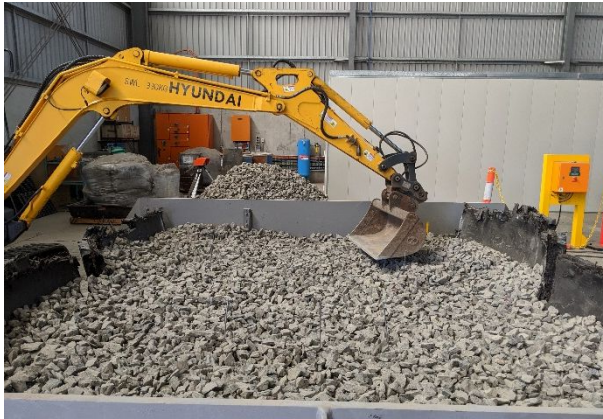
(c)

(d)

(e)

(f)

Figure 6. Preparing the CCT: (a) sand-cone test on the capping layer (b) installing the tyre arch segments followed by ballast filling (c) placing the load-bearing ballast to a thickness of 300 mm (d) placing the sleeper-rail assembly with the aid of an overhead crane (e)

compaction of crib ballast, and (f) installing the loading frame and actuators using the

overhead crane
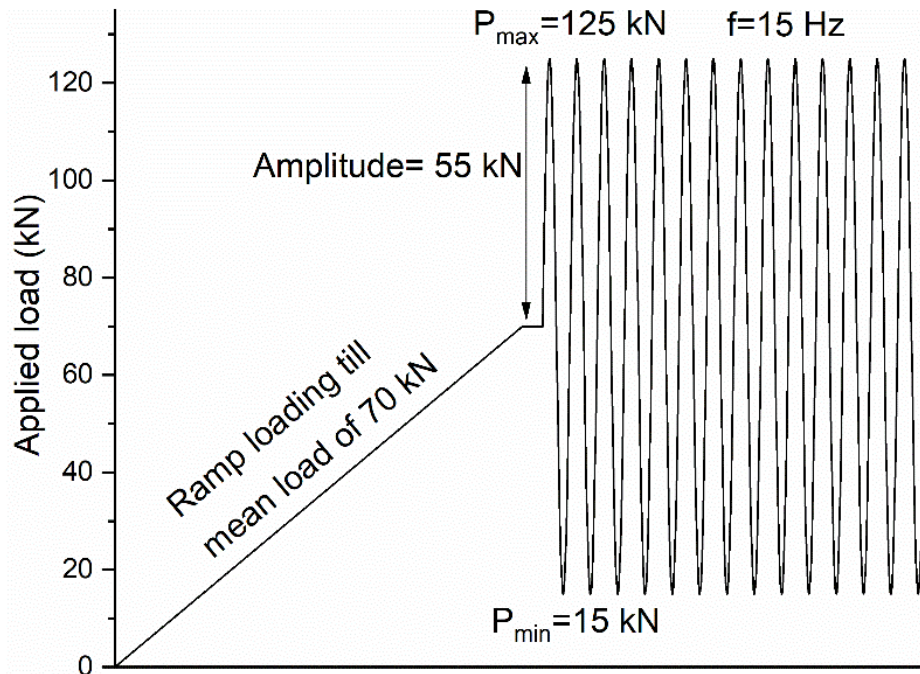
Figure 7. Loading program for a typical cyclic test
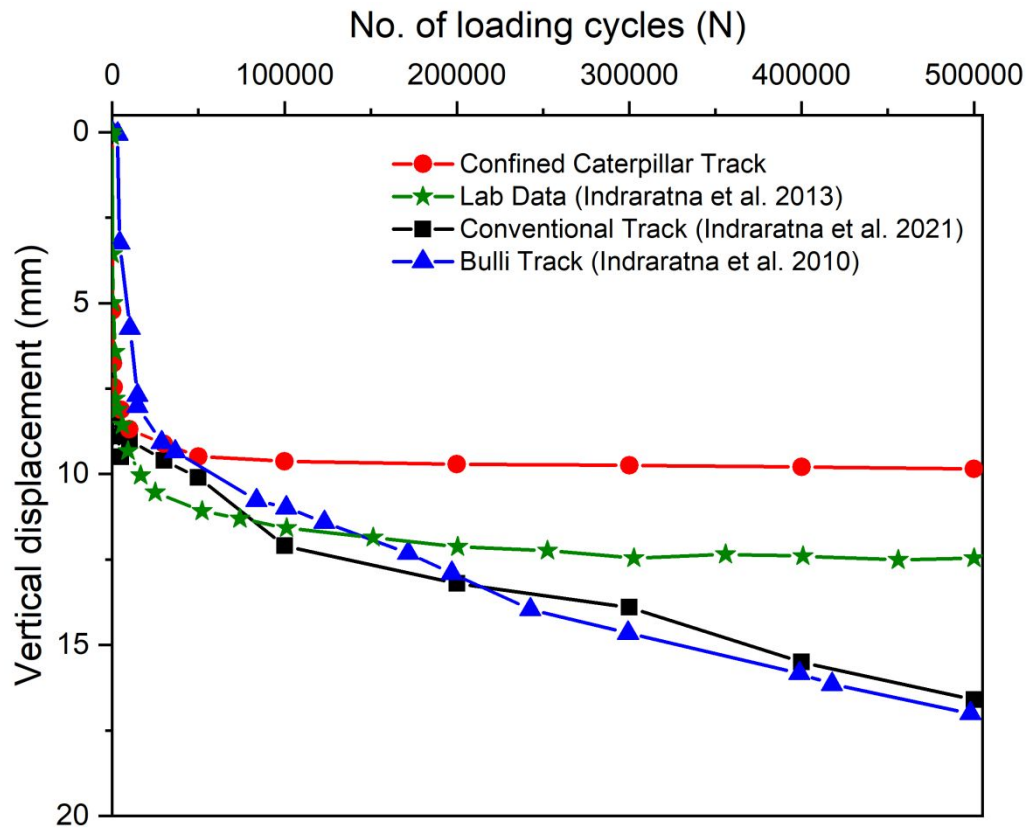
Figure 8. Vertical settlements of CCT under cyclic loading
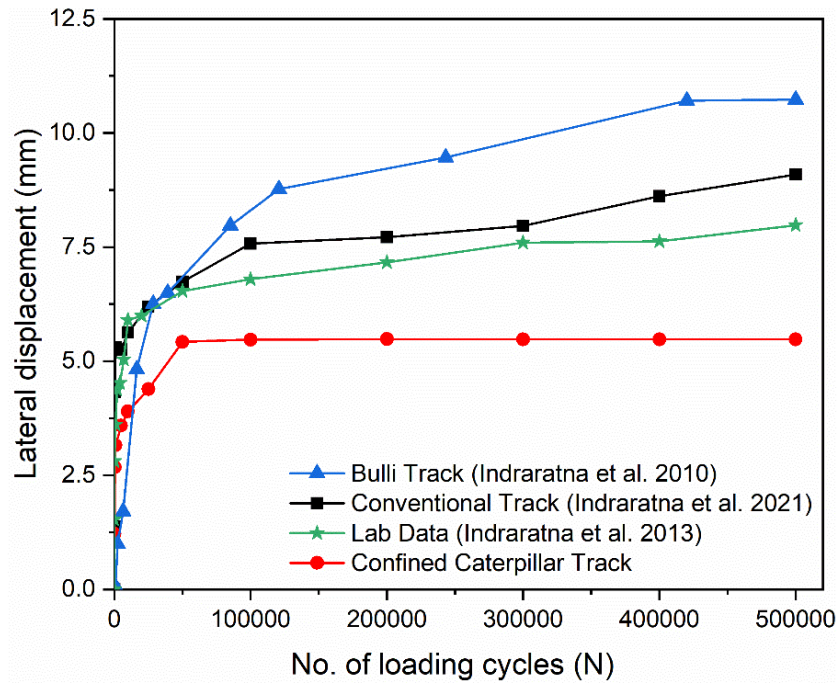
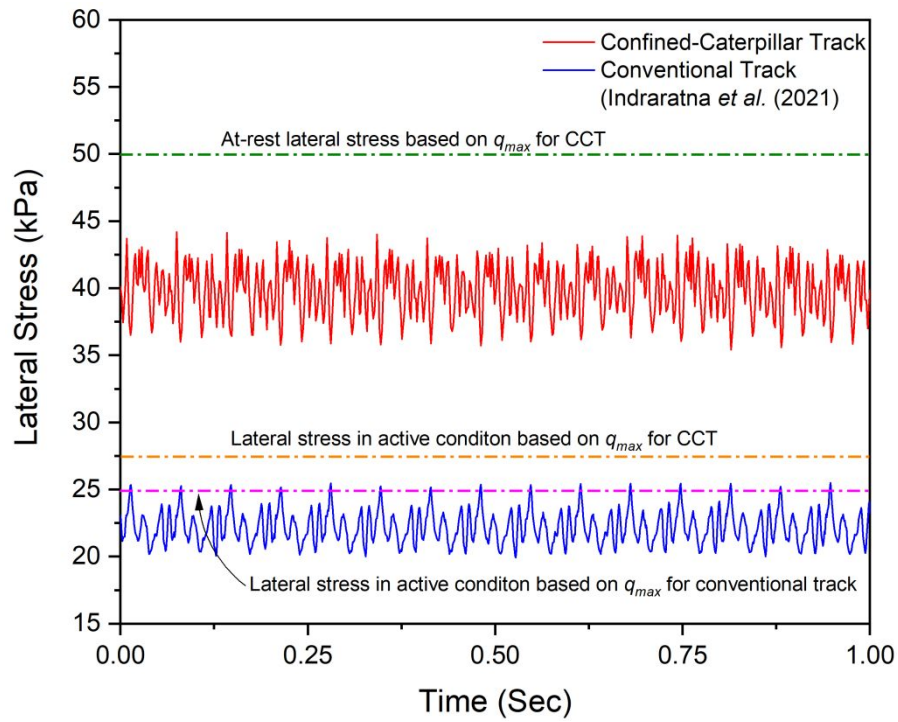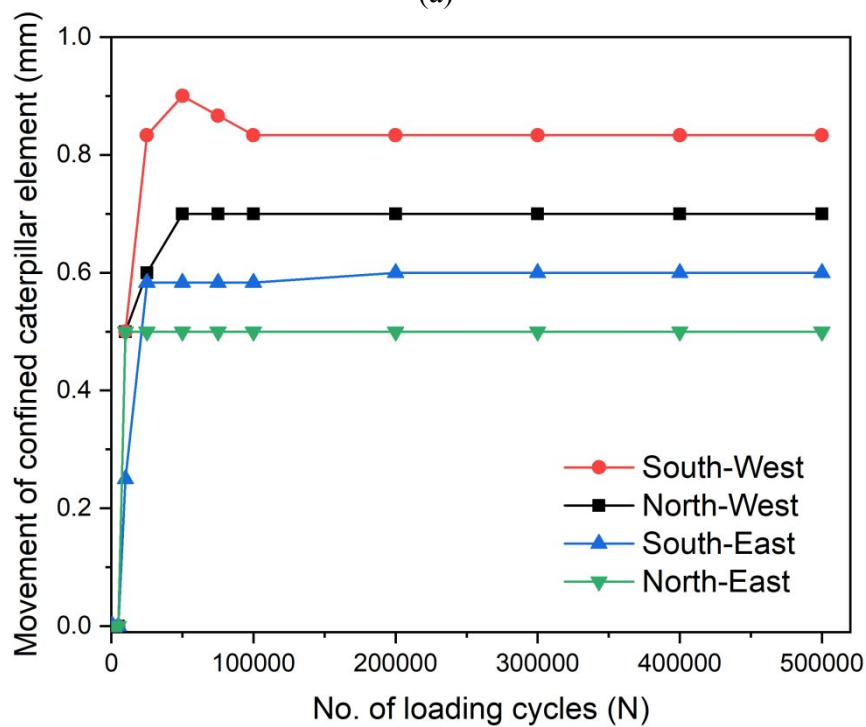**Figure 9.** Lateral movements of CCT under cyclic loading
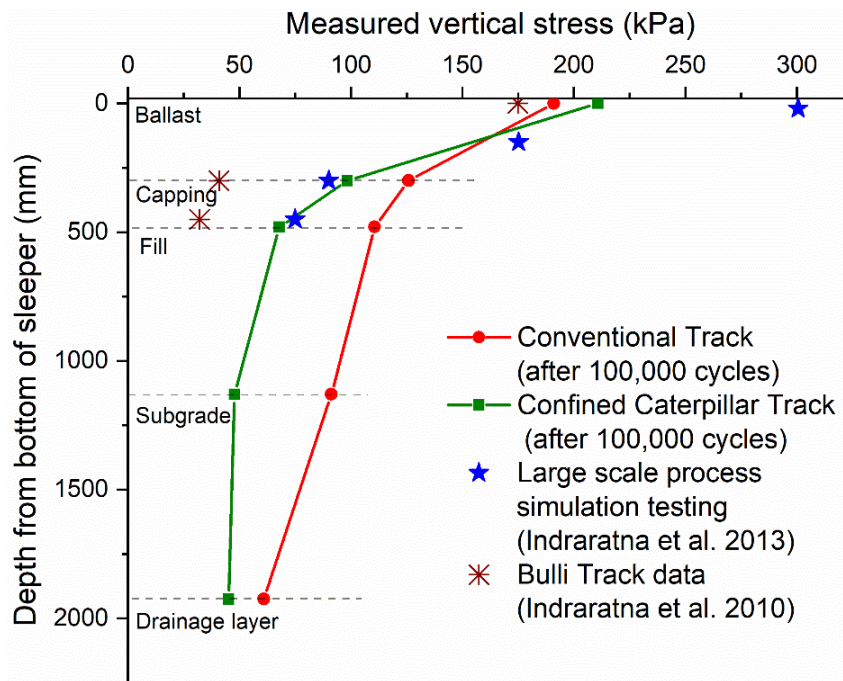
(a)
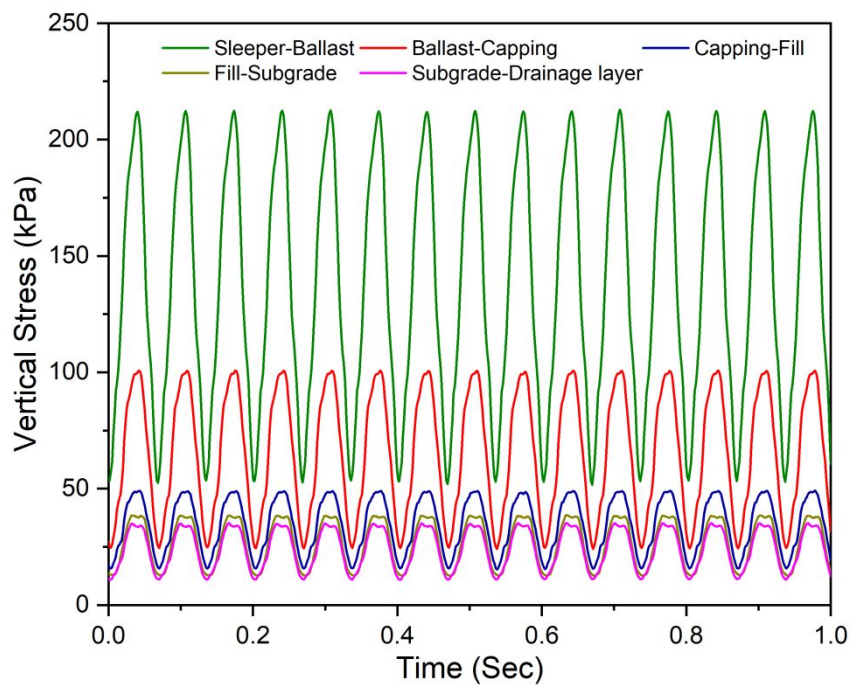
(b)

Figure 10. (a) Stress distributions along the depth after 100,000 cycles of loading and (b)

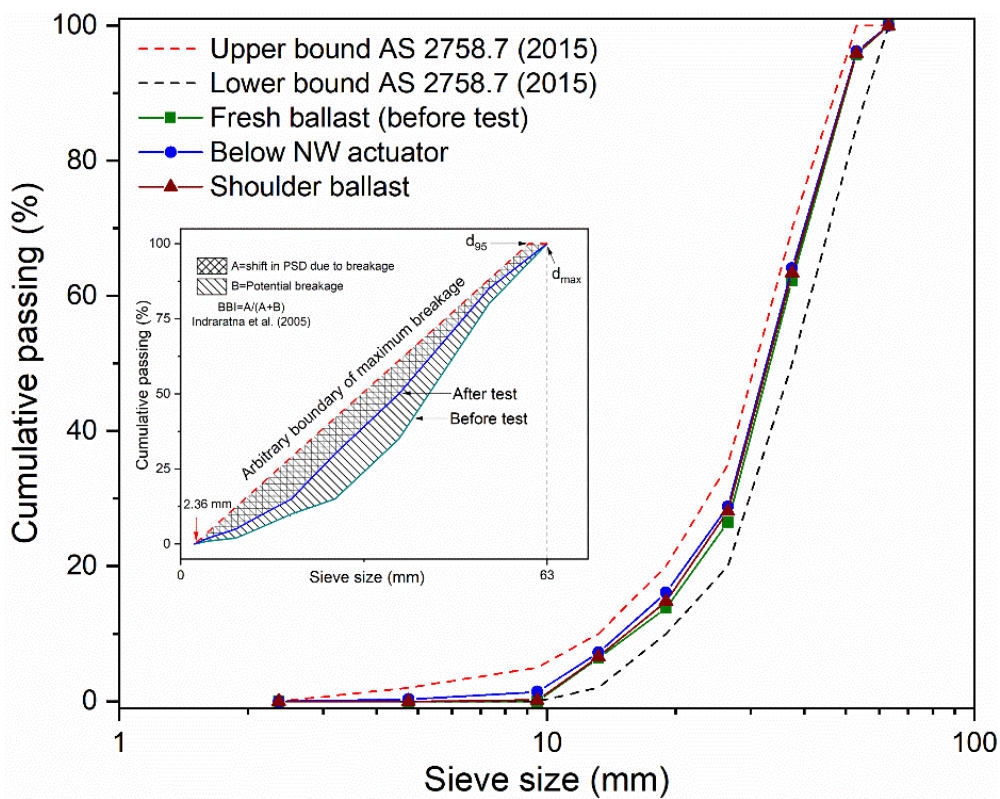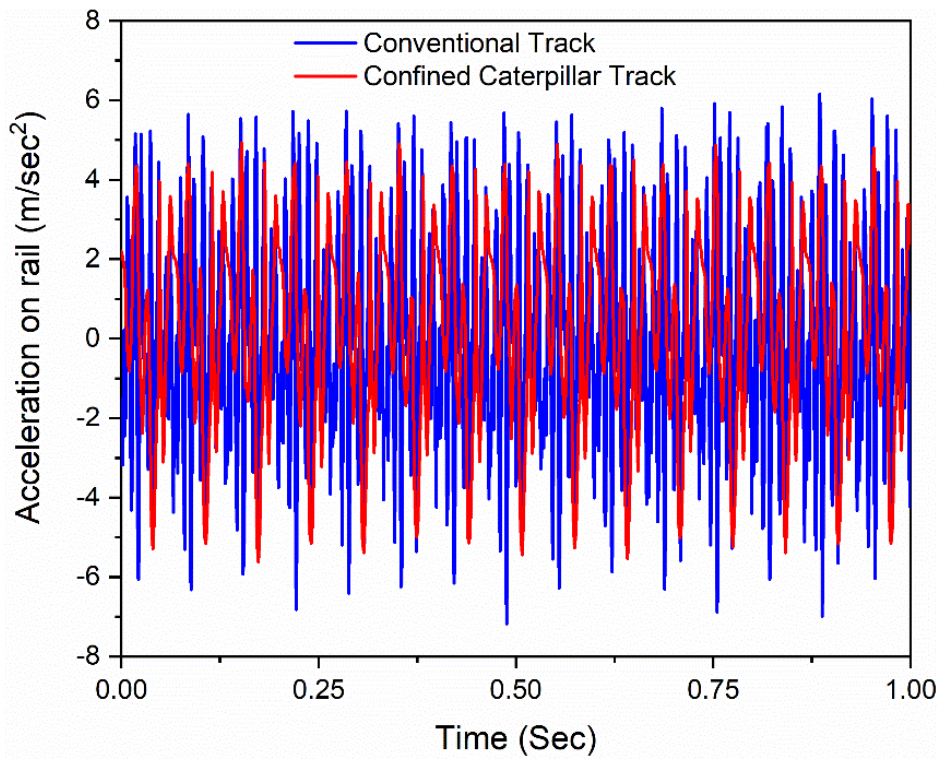cyclic deviatoric stresses at different depths measured for the CCT track

(a)

(b)

Figure 11. (a) Lateral stress generated in the ballast layer for the conventional track and

CCT, and (b) movement of the tyre elements during testing

44

Figure 12. Particle size gradation before and after testing and ballast breakage analysis

Figure 13. Measured accelerations on the steel rail